https://doi.org/10.5194/egusphere-2026-5194
Preprint. Discussion started: 4 September 2026

Multifractal characterization of daily maximum and minimum ionospheric TEC at African equatorial stations

Babatunde Rabiu[1,2], Samuel Ogunjo[2,3], and Ayomide Olabode[4,5]

[1]Institute of Space Science and Engineering, African University of Science and Technology, 900107 Abuja, Nigeria
[2]Network of Space-Earth Environmentalists, 900107 Abuja, Nigeria
[3]Department of Physics, Federal University of Technology Akure, 340252 Akure, Nigeria
[4]Institut fur Geodesie und Geoinfomationstechnik, Technische Universitat Berlin, 10553 Berlin, Germany
[5]Department of Physics and Engineering Physics, Obafemi Awolowo University, 220282 Ile-Ife, Nigeria

Correspondence: Samuel Ogunjo (stogunjo@futa.edu.ng)

Abstract. The temporal scaling structure of the ionospheric vertical total electron content (vTEC) carries fundamental information about the intrinsic dynamics of the equatorial and low-latitude plasma system. This study applies Multifractal Detrended Fluctuation Analysis (MFDFA) to investigate the intrinsic dynamics of the variability of the ionosphere over African equatorial stations using the daily maximum and minimum vTEC time series recorded at three GNSS stations (Dakar (DAKR), Libreville (NKLG), and Djibouti (DJIG) spanning the equatorial ionisation anomaly (EIA) crest and its flanks. Seasonal trend components are isolated using Seasonal and Trend decomposition with Loess (STL) to separate the contribution of the seasonal cycle from intrinsic ionospheric dynamics. The raw maximum vTEC series exhibit clear semi-annual modulation and multifractality at all stations, with generalised Hurst exponents $0.104 \leq h(q=2) \leq 0.193$ and statistically significant singularity spectral widths. A crossover in scaling behaviour near $n \approx 150$ days reveals scale-dependent persistence that is stronger at sub-annual scales. The raw minimum vTEC series confirm multifractality but with consistently narrower singularity spectra and weaker q-dependence, reflecting the reduced dynamic range of the nighttime ionosphere in the absence of photo-ionisation. These results reveal a clear daytime-nighttime asymmetry in ionospheric scaling dynamics and establish the EIA crest as a region of persistent, non-seasonal nonlinear variability that manifests across both the daytime and nighttime ionosphere. The findings demonstrate that MFDFA applied to the diurnal extremes of vTEC provides a sensitive and physically interpretable diagnostic of equatorial ionospheric complexity that is not accessible through conventional spectral or trend-based analyses.

1 Introduction

Ionospheric electron density is continuously modified by solar radiative forcing, solar-wind–magnetosphere coupling, neutral-atmospheric dynamics, electrodynamic transport, and plasma-chemical processes (Hargreaves, 1992; Rishbeth, 1998; Kelley, 2009; Schunk and Nagy, 2009). Upward coupling from atmospheric sources (Lieberman et al., 2026; Nanda et al., 2026) and,

https://doi.org/10.5194/egusphere-2026-5194
Preprint. Discussion started: 4 September 2026

under specific geophysical conditions, lithosphere–atmosphere–ionosphere coupling (Pulinets and Dimitar, 2011; Kuo et al., 2014; Adebayo et al., 2025; Obasanjo et al., 2026) may further modulate ionospheric variability.

Vertical total electron content (TEC), derived from dual-frequency Global Navigation Satellite System (GNSS) observations, provides an integrated measure of ionospheric electron density and is widely used to monitor ionospheric variability and its effects on trans-ionospheric signals (Mannucci et al., 1998; Schaer, 1999; Hernández-Pajares et al., 2009; Jakowski et al., 2011). At equatorial and low-latitudes (include spatial extent), TEC variability is strongly shaped by solar photoionisation, recombination, neutral winds, electric fields, and the equatorial fountain process, which produces the equatorial ionization anomaly (EIA) (Appleton, 1946; Moffett and Hanson, 1965; Hanson and Moffett, 1966; Anderson, 1973; Balan et al., 2018). Consequently, GNSS stations located within the equatorial and low-latitude can exhibit substantially different TEC amplitudes, gradients, and temporal variability.

The African equatorial and low-latitude ionosphere is an important region for analysing vTEC variability because it spans a broad and persistent footprint of the EIA while remaining less densely monitored than many other longitude sectors. Previous studies have documented strong diurnal, seasonal, latitudinal, longitudinal, and solar-cycle dependence of TEC variability over Africa (Akala et al., 2013; Opio et al., 2015; Olwendo et al., 2016; Andima et al., 2019; Okoh et al., 2019; Ogwala et al., 2022). Event-based studies have further shown that transient external forcing, including geomagnetic storms and solar eclipses, can produce substantial TEC and scintillation responses over Africa (e.g., Okoh et al., 2020; Olabode and Ariyibi, 2020; Uga et al., 2024; Muniafu et al., 2026). The amplitude, timing, and recovery of these responses depend on latitude, longitude, local time, season, storm intensity and phase, and, for eclipses, the magnitude and duration of solar obscuration. These studies have established the broad climatological and disturbed-time behaviour of the African ionosphere, but most have relied on mean behaviour, anomalies, occurrence statistics, or spectral descriptions. Such approaches do not fully quantify how TEC fluctuations of different amplitudes are organised across temporal scales.

This distinction is important because similar seasonal or semiannual behaviour in vTEC does not necessarily imply similar fluctuation dynamics. A station may exhibit a largely smooth seasonal signal, whereas another may show comparable background modulation interrupted by storm-time enhancements, depletions, or transient electrodynamic disturbances (Mendillo, 2006). MFDFA addresses this problem by estimating the dependence of fluctuation scaling on moment order, allowing weak and intense fluctuations to be characterised separately in nonstationary geophysical time series (Halsey et al., 1986; Peng et al., 1994; Kantelhardt et al., 2002; Kantelhardt, 2009). Recent geospace applications have shown that multifractal and nonlinear measures can reveal dynamical structure in geomagnetic activity and storm recurrence that is not captured by conventional linear descriptors alone (Ogunjo et al., 2024a, b, 2021).

Previous applications of multifractal methods to ionospheric TEC have shown that TEC fluctuations do not scale uniformly across time, and that their scaling behaviour varies with latitude, solar activity, geomagnetic conditions, season, and local time (Bolzan et al., 2013; Tanna and Pathak, 2014b, a; Chandrasekhar et al., 2016; Sivavaraprasad et al., 2018; Bhardwaj et al., 2020; Momeni and Migoya-Orué, 2026). However, the multifractal properties of daily maximum and daily minimum TEC have not been comparitvely investigated as a representation of daytime and nighttime ionospheric conditions, respecitviely, particularly over the African EIA sector. This comparison is physically meaningful because the daily maximum vTEC is usually

https://doi.org/10.5194/egusphere-2026-5194
Preprint. Discussion started: 4 September 2026

associated with the daytime ionosphere, when photoionisation, F-region plasma production, thermospheric composition, and fountain-driven redistribution dominate. The daily minimum vTEC is more closely associated with the nighttime or pre-dawn ionosphere, when direct solar production is absent and electron density is controlled more strongly by recombination, transport, neutral winds, plasmaspheric exchange, and residual electrodynamics (Rishbeth, 1998; Kelley, 2009; Schunk and Nagy, 2009; Balan et al., 2018).

A further challenge is that vTEC contains strong annual and semi-annual components that can themselves impose apparent scaling structure. If these components are not treated explicitly, multifractal parameters estimated from raw vTEC series may conflate regular seasonal modulation with residual nonlinear variability. Seasonal and Trend decomposition using Loess (STL) provides a means of separating seasonal, trend, and residual components (Cleveland et al., 1990). Applying MFDFA to both raw and STL-detrended vTEC therefore allows the seasonal contribution to the scaling structure to be assessed separately from the scaling behaviour retained by the residual signal. Surrogate testing further helps determine whether the observed multifractality exceeds that expected from linear correlations and amplitude distribution only (Theiler et al., 1992; Schreiber and Schmitz, 1996).

This study applies MFDFA to daily maximum and daily minimum vTEC time series from three African equatorial GNSS stations with a view to characterising the multifractal scaling properties of the daytime and night-time ionosphere across the equatorial ionisation anomaly (EIA) crest and its flanks, and to establishing the extent to which this scaling structure is intrinsic to the underlying plasma dynamics rather than inherited from the dominant seasonal and diurnal cycle. To this end, both raw and STL-detrended series spanning 2017–2019 are analysed, allowing the generalised Hurst exponent, singularity spectrum width, and spectral asymmetry to be compared across stations, between daily maximum and minimum, and before and after trend removal. The remainder of this paper is organised as follows: Section 2 presents the data and methodology employed in this study, while Section 3 discusses the results obtained from the various analyses undertaken, including the daily maximum-minimum asymmetry in scaling behaviour.

2 Methodology

2.1 Study area and data

Daily maximum and minimum vertical total electron content (vTEC) values were obtained at three stations: Dakar (DAKR), Nkalagu (NKLG), and Djibouti (DJIG), spanning the period 2017–2019 (Figure 1). The type of data transformation during detrending has effect on the outcome of dynamical analysis (Ogunjo, 2015), hence the need for caution in detrending. Detrending of the raw data was carried out using seasonal-trend decomposition with LOESS (STL) interpolation (Cleveland et al., 1990) prior to analysis. This approach preserves the structure and nature of the underlying data. Each time series was decomposed with a periodic window of 24, yielding a seasonal component, a smooth trend, and a residual (detrended) series (Cleveland et al., 1990). Both the raw and detrended vTEC series were retained for independent multifractal analysis, allowing the contribution of seasonal structure to the scaling properties to be assessed.

https://doi.org/10.5194/egusphere-2026-5194
Preprint. Discussion started: 4 September 2026

Table 1. Geographic and geomagnetic coordinates of the GNSS stations used in the study. Geomagnetic coordinates are approximate centered-dipole coordinates.

Station	Location	Geographic coordinates		Geomagnetic coordinates	
		Latitude (°)	Longitude (°)	Latitude (°)	Longitude (°)
DAKR	Dakar, Senegal	14.721	-17.439	2.35	57.91
NKLG	Libreville, Gabon	0.354	9.672	-8.04	81.05
DJIG	Djibouti City, Djibouti	11.526	42.847	3.33	114.57

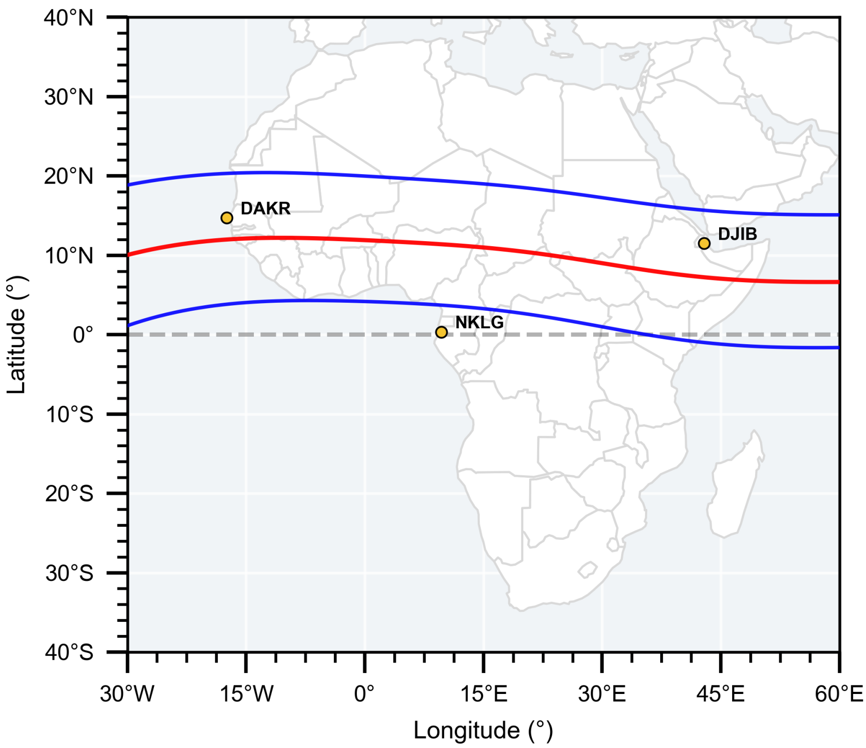

Figure 1. Geographic distribution of the three African GNSS stations used in this stud, spanning longitudes from West Africa to East Africa and sampling different portions of the equatorial and low-latitude ionosphere. The dashed grey line represents the geographic equator. The red curve denotes the magnetic equator, while the blue curves indicate the approximate northern and southern magnetic latitudes bounding the equatorial ionisation anomaly (EIA) region.

https://doi.org/10.5194/egusphere-2026-5194
Preprint. Discussion started: 4 September 2026

2.2 Multifractal Detrended Fluctuation Analysis

Multifractal detrended fluctuation analysis (MFDFA) (Kantelhardt et al., 2002) was applied to both raw and detrended vTEC series using the `fathon` Python library (Bianchi, 2020). For each series $x(i)$ of length N, the mean-subtracted profile is formed as

$$Y(i) = \sum_{k=1}^{i} \left[x(k) - \langle x \rangle\right], \quad i = 1, \ldots, N. \tag{1}$$

The profile is divided into $N_s = \lfloor N/s \rfloor$ non-overlapping segments of length s, and the procedure is repeated from the end of the series to ensure full coverage (reversed segmentation). Within each segment ν, a polynomial trend of order $m = 1$ is fitted and subtracted, and the local variance is computed. The qth-order fluctuation function is then

$$F_q(s) = \left\{ \frac{1}{2N_s} \sum_{\nu=1}^{2N_s} \left[F^2(\nu, s)\right]^{q/2} \right\}^{1/q}, \tag{2}$$

where the special case $q = 0$ is evaluated via the logarithmic average (Kantelhardt et al., 2002). Window sizes were varied over the range $s \in [50, 1000]$ in uniform steps, and moment orders were set to $q \in [-3, 4]$ at intervals of 0.1, giving 71 values of q. If the series possesses multifractal scaling, $F_q(s)$ follows a power law

$$F_q(s) \sim s^{h(q)}, \tag{3}$$

where $h(q)$ is the generalised Hurst exponent. For each value of q, $h(q)$ was estimated by ordinary least-squares regression of $\ln F_q(s)$ on $\ln s$ over the full scale range. To investigate potential crossover behaviour, the log-log range was additionally divided at the midpoint (s_{mid}), and separate slopes $h_1(q)$ and $h_2(q)$ were estimated for the small-scale and large-scale regimes, respectively.

The mass exponents $\tau(q)$ were obtained from the generalised Hurst exponents as

$$\tau(q) = q\,h(q) - 1. \tag{4}$$

The singularity spectrum $f(\alpha)$ was derived via the Legendre transform

$$\alpha = \frac{\mathrm{d}\tau}{\mathrm{d}q}, \tag{5}$$

$$f(\alpha) = q\,\alpha - \tau(q), \tag{6}$$

yielding the Hölder exponent α and the fractal dimension of the subset carrying that exponent (Feder, 2013; Halsey et al., 1986). Three scalar descriptors were extracted from the spectrum: (i) the dominant singularity exponent $\alpha_0 = \alpha\big|_{\max f(\alpha)}$, which corresponds to the most frequently occurring scaling behaviour; (ii) the spectral width $\Delta\alpha = \alpha_{\max} - \alpha_{\min}$, a measure of the overall degree of multifractality; and (iii) the asymmetry index

$$r = \frac{\alpha_{\max} - \alpha_0}{\alpha_0 - \alpha_{\min}}, \tag{7}$$

https://doi.org/10.5194/egusphere-2026-5194
Preprint. Discussion started: 4 September 2026

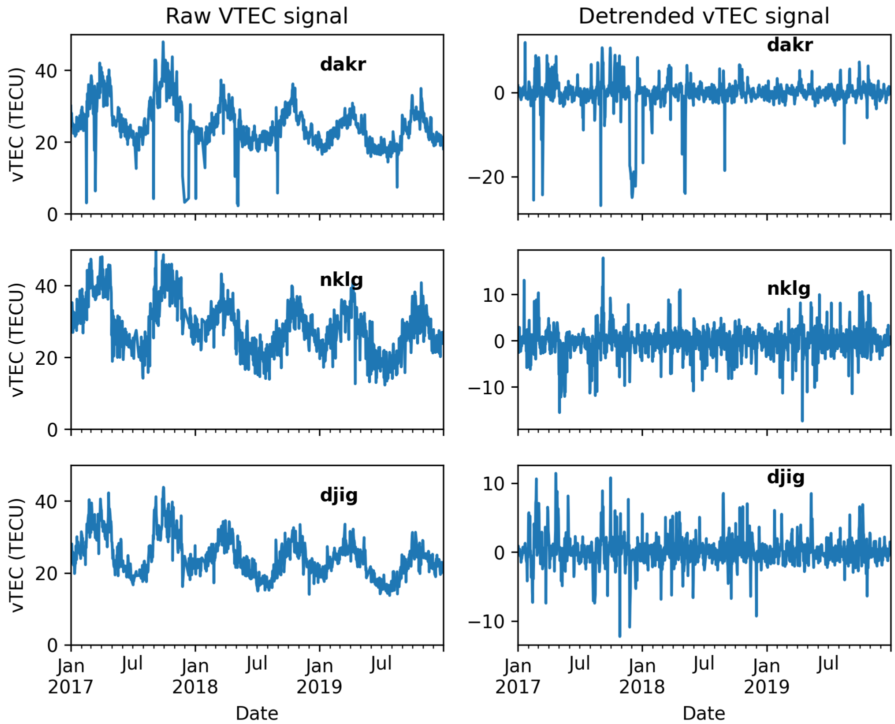

Figure 2. Time series of daily maximum vertical total electron content (vTEC) at three GNSS stations (DAKR, NKLG, DJIG) over the period January 2017 to December 2019. Left panels show the raw vTEC signal; right panels show the corresponding STL-detrended residuals after removal of the seasonal trend component.

where $r > 0$ indicates dominance of large fluctuations (right-skewed spectrum) and $r < 0$ indicates dominance of small fluctuations (Shimizu et al., 2002).

To distinguish multifractality arising from long-range temporal correlations from that arising from a broad (fat-tailed) probability distribution, Amplitude-Adjusted Fourier Transform (AAFT) surrogates were employed (Theiler et al., 1992; Schreiber and Schmitz, 1996). For each observed series, $n = 10$ AAFT surrogate realisations were generated. Each surrogate preserves the power spectrum (and hence the linear autocorrelation structure) and the amplitude distribution of the original series, but destroys nonlinear temporal dependencies (Theiler et al., 1992). MFDFA was applied to all surrogates, and the mean $\bar{\Delta\alpha}$ and standard deviation $\sigma_{\Delta\alpha}$ of the spectral width were computed. The standardised deviation

$$S = \frac{\Delta\alpha - \bar{\Delta\alpha}}{\sigma_{\Delta\alpha}} \tag{8}$$

quantifies how many standard deviations the observed multifractality exceeds that of the linear surrogates; a large positive $S > 2$ indicates that nonlinear temporal correlations, rather than the marginal distribution alone, are the primary source of multifractality (Kantelhardt et al., 2002; Theiler et al., 1992).

https://doi.org/10.5194/egusphere-2026-5194
Preprint. Discussion started: 4 September 2026

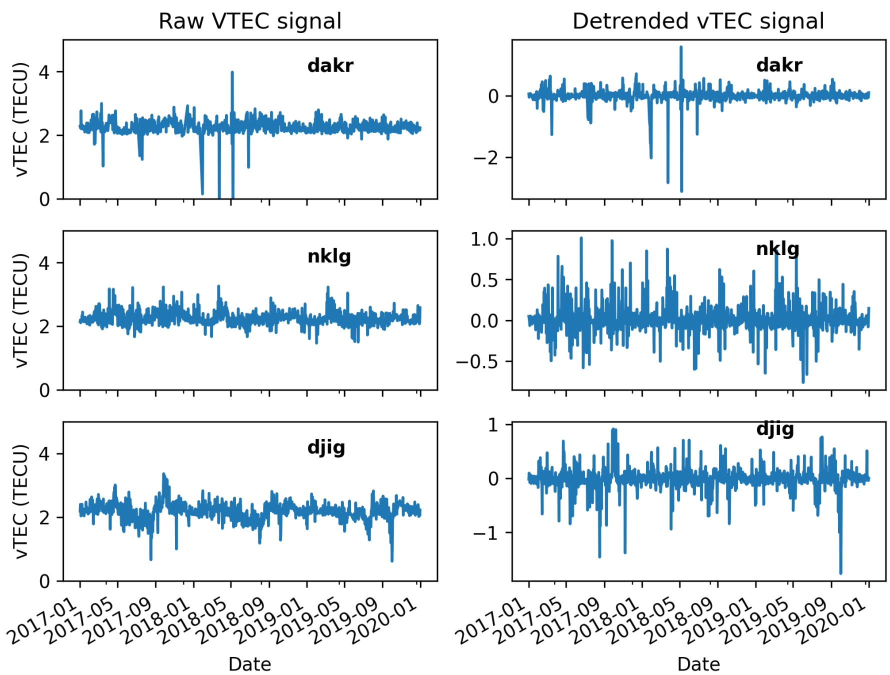

Figure 3. Time series of daily minimum vertical total electron content (vTEC) at three GNSS stations (DAKR, NKLG, DJIG) over the period January 2017 to December 2019. Left panels show the raw vTEC signal; right panels show the corresponding STL-detrended residuals after removal of the seasonal trend component.

3 Results and discussion

Figure 2 and Figure 3 present the daily maximum and minimum vTEC time series, respectively, for the three GNSS stations over 2017–2019, with the respective STL-detrended time series. These plots reveal a striking contrast in ionospheric dynamics between the daytime and nighttime ionosphere across the study region. The raw maximum vTEC series show clear semi-annual modulation at all three stations. Amplitude peaks occur during the March and September equinoctial periods, consistent with the well-documented influence of solar zenith angle and thermospheric composition on the equatorial and low-latitude ionosphere (Rishbeth, 1998; Liu et al., 2006). The raw minimum vTEC time series reflect the nighttime ionosphere, where photo-ionisation is absent and plasma density is governed by recombination and transport processes (Kelley, 2009). Accordingly, the minimum series show markedly lower absolute values, typically between 2 and 4 TECU, and a much weaker seasonal signal at all three stations. Within the maximum series, Dakar (DAKR) records the largest absolute values, exceeding 40 TECU during equinoctial maxima. This is attributable to its proximity to the equatorial ionisation anomaly (EIA) trough. Nkalagu (NKLG) and Djibouti (DJIG) are also near-equatorial stations and display similarly elevated but slightly subdued levels. Detrending sharpens these inter-station contrasts considerably. In the maximum series, detrended vTEC at DAKR retains high-amplitude transients with negative excursions exceeding −20 TECU. These are largely absent or much weaker at

https://doi.org/10.5194/egusphere-2026-5194
Preprint. Discussion started: 4 September 2026

NKLG, and DJIG, whose residuals remain confined within ±15 TECU. This pattern is indicative of localised ionospheric depletion events and plasma bubble activity that are disproportionately prevalent in the West African sector (Abdu, 2012). It also suggests that the dominant source of high-frequency variability at DAKR is not purely seasonal but reflects the strongly nonlinear dynamics of equatorial plasma irregularities. In the minimum series, the detrended amplitudes at NKLG, and DJIG collapse to within ±1 TECU. This is a reduction of more than an order of magnitude relative to the maximum residuals and underscores the reduced dynamic range of the nighttime ionosphere. The detrended minimum residuals at DAKR was found to descend below -2 TECU, with sharp negative spikes falling below 1 TECU during 2018. These are likely associated with severe nighttime depletion events or sporadic-E layer interference. The temporal clustering of these excursions during 2017 and 2018 points to a geomagnetic or solar-cycle modulation of nighttime plasma depletion during the descending phase of Solar Cycle 24 (Adebesin et al., 2015). The maximum and minimum vTEC records establish DAKR as the most dynamically active station in the network, with non-seasonal variability that is larger in magnitude and qualitatively distinct from the other three stations across both the daytime and nighttime ionosphere.

Figures 4 and 5 present the MFDFA log-log fluctuation functions $\ln F_q(n)$ versus $\ln(n)$ for the raw and detrended daily maximum and minimum vTEC series, respectively, at $q \in \{-3, 2, 4\}$. In the raw maximum series, a clear separation of the scaling lines by q-order is visible at all three stations. The $q = -3$ line exhibits the steepest slope and the $q = 4$ line the shallowest, confirming genuine multifractal scaling in which the generalised Hurst exponent $h(q)$ decreases with increasing q (Kantelhardt et al., 2002). The raw minimum series also show q-separation, but it is notably weaker at NKLG, and DJIG, indicating reduced multifractality in the nighttime ionosphere. This is consistent with the tabulated values (Table 2), where $h_{\mathrm{full}}(q = 2)$ ranges from 0.104 to 0.193 for the raw maximum series but only from 0.020 to 0.046 for the raw minimum series. DAKR is the exception, retaining the greatest q-separation in both series, with $h_{-3} = 0.27$ and $h_4 = -0.06$ for the raw minimum. A crossover in scaling behaviour is apparent in the log-log plots of the maximum series, particularly at DAKR and DJIG, near $\ln(n) \approx 5$ (i.e. $n \approx 150$ days), suggesting a transition between dynamical regimes at sub-annual scales. This feature is reflected in the first and second half slopes reported in Table 2. At DAKR, for example, $h_1 = 0.306$ and $h_2 = 0.044$, indicating that persistence is stronger at smaller scales. The crossover is less pronounced in the minimum series, and scaling is generally more uniform across the full scale range, suggesting that nighttime vTEC lacks the scale-dependent memory structure present in the daytime maximum. The crossover remains discernible in the minimum series at DAKR near $\ln(n) \approx 5$, though it is less sharp than in the maximum case. The $h_{\mathrm{full}}(q = 2)$ values for the raw maximum series at DAKR, NKLG, and DJIG are 0.127, 0.104, 0.182, and 0.193, respectively. All lie below 0.5, indicating anti-persistent short-range correlations in the raw maximum vTEC fluctuations. The corresponding values for the raw minimum series are smaller and closer to zero, further confirming weaker temporal memory in the nighttime ionosphere. Following STL detrending, the scaling functions in the maximum series collapse to near-horizontal lines at NKLG, and DJIG, with h_{full} approaching zero or becoming slightly negative. This indicates that once the seasonal trend is removed, the residuals carry no significant long-range memory at these stations. DAKR alone retains a positive $h_{\mathrm{full}} = 0.041$ after detrending, reflecting the persistence of high-amplitude transient depletions that seasonal decomposition cannot capture. In the minimum series, detrending reduces the fluctuation functions to near-horizontal lines at all three stations, with detrended $h(q = 2)$ values lying between -0.002 and 0.031. This confirms that

https://doi.org/10.5194/egusphere-2026-5194
Preprint. Discussion started: 4 September 2026

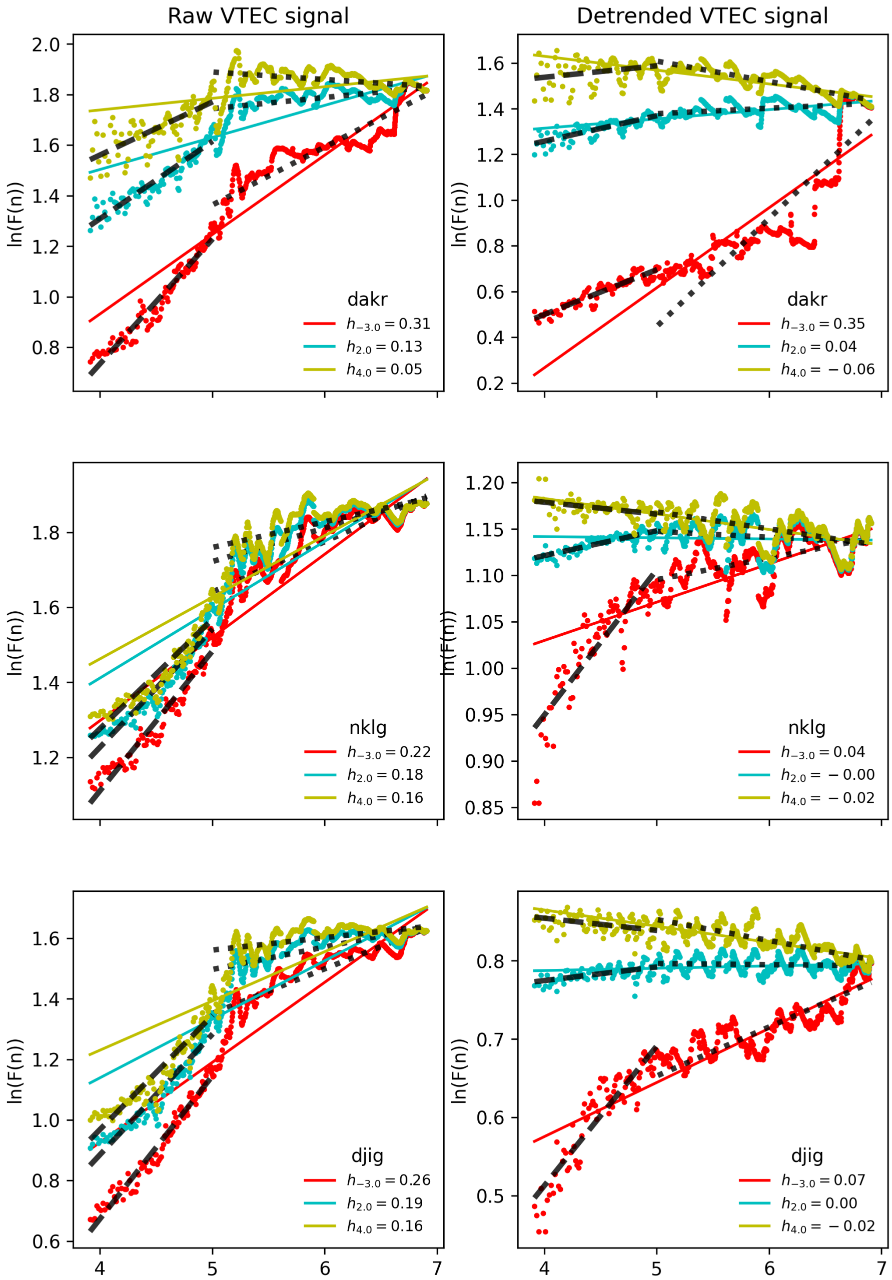

Figure 4. Log-log fluctuation functions $\ln F_q(n)$ versus $\ln(n)$ obtained from multifractal detrended fluctuation analysis (MFDFA) of the daily maximum vTEC series at DAKR, NKLG, and DJIG. Left panels correspond to the raw signal; right panels to the STL-detrended series.

virtually all long-range scaling in the minimum series is carried by the seasonal trend component rather than by the underlying

https://doi.org/10.5194/egusphere-2026-5194
Preprint. Discussion started: 4 September 2026

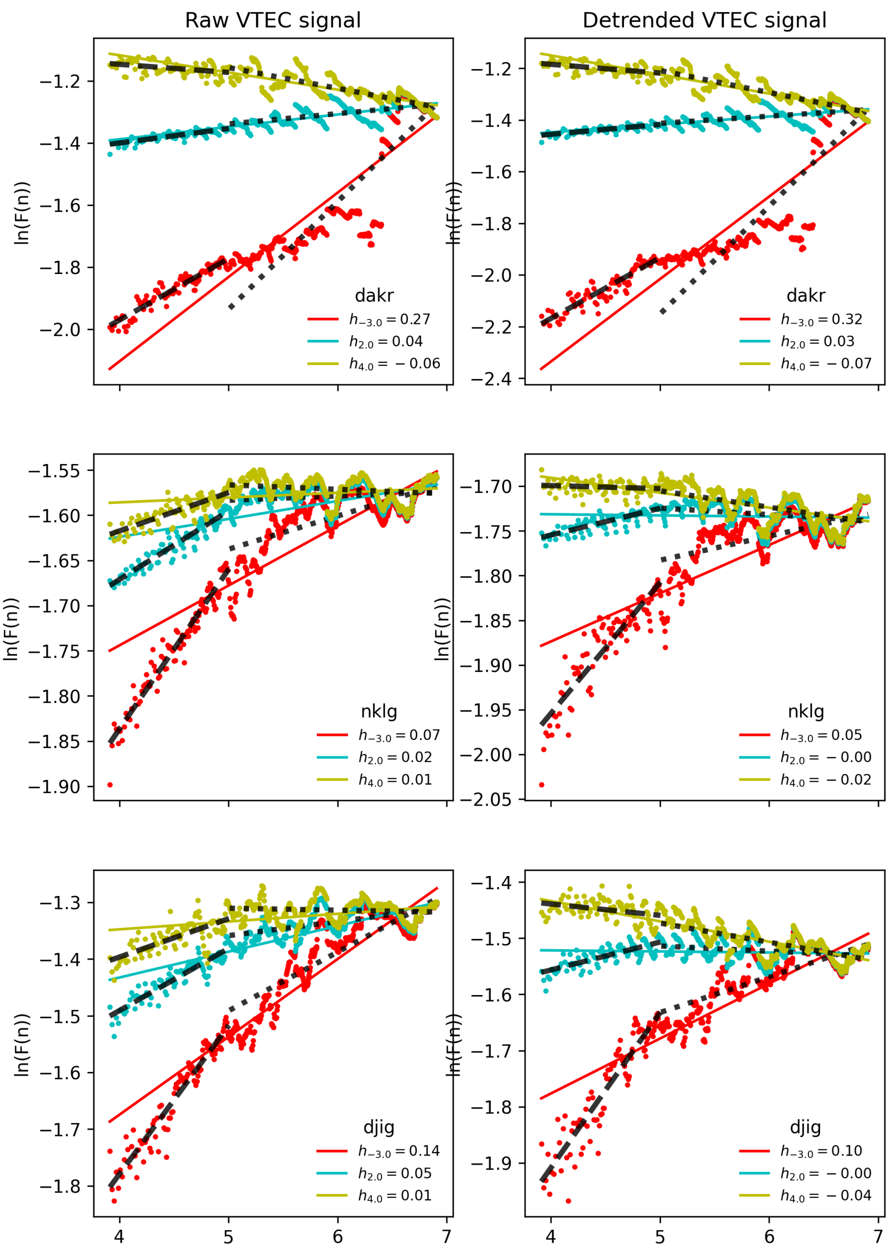

Figure 5. Log-log fluctuation functions $\ln F_q(n)$ versus $\ln(n)$ obtained from multifractal detrended fluctuation analysis (MFDFA) of the daily minimum vTEC series at DAKR, NKLG, and DJIG. Left panels correspond to the raw signal; right panels to the STL-detrended series.

residual dynamics, a stark contrast to DAKR in the maximum series and consistent with the reduced dynamic range of the nighttime ionosphere established in Figure 5.

https://doi.org/10.5194/egusphere-2026-5194
Preprint. Discussion started: 4 September 2026

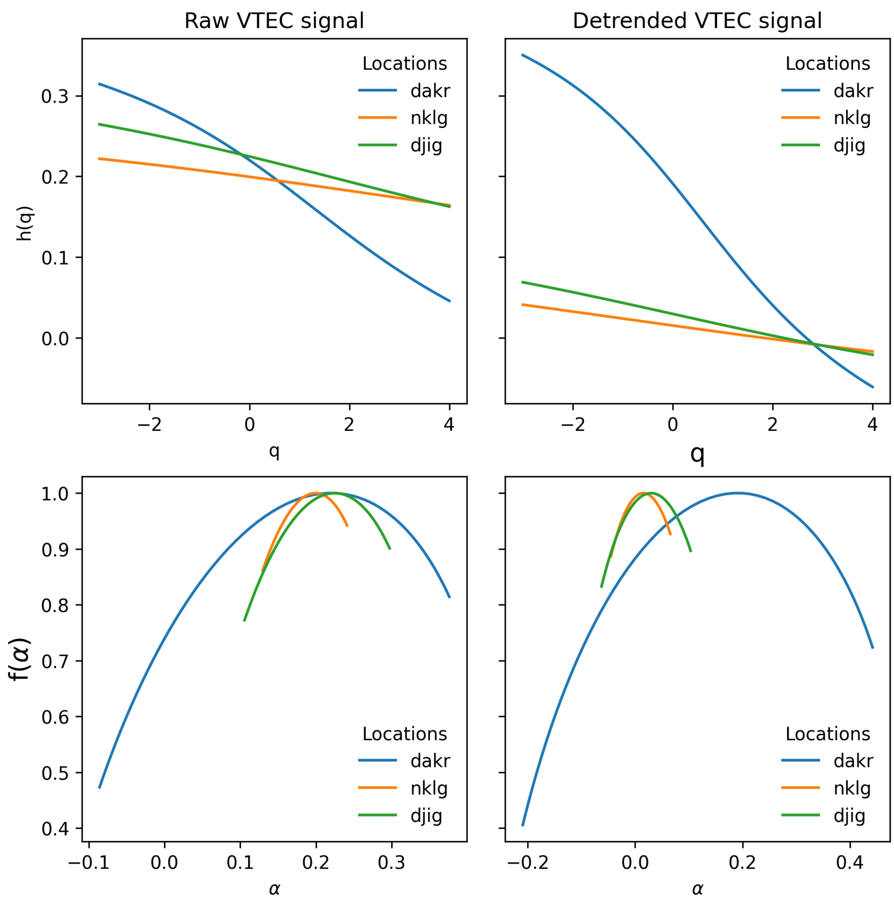

Figure 6. Multifractal scaling characteristics of daily maximum vTEC derived from MFDFA at the three GNSS stations. Upper panels: generalised Hurst exponent $h(q)$ as a function of moment order $q \in [-3, 4]$ for the raw (left) and STL-detrended (right) series. Lower panels: corresponding multifractal singularity spectra $f(\alpha)$ versus Hölder exponent α for the raw (left) and detrended (right) series.

Figures 6 and 7 display the q-dependence of the generalised Hurst exponent $h(q)$ and the corresponding multifractal singularity spectra $f(\alpha)$ for the raw and detrended daily maximum and minimum vTEC series, respectively. In both series, $h(q)$ decreases monotonically with q at all stations, confirming multifractality. For both the raw and detrended series, and in both the daily maximum and minimum VTEC data, the generalized Hurst exponent at $q = 2$ was found to satisfy $h(2) < 0.5$. An $h(2)$ value below 0.5 indicates that the vTEC series is anti-persistent rather than persistent which implies that large values tend to be followed by small ones and vice versa, so the fluctuations show a self-correcting, mean-reverting behaviour rather than sustained trends. Since this holds consistently across raw and detrended data, and for both maximum and minimum series, it suggests that anti-persistence is a robust, underlying feature of the ionospheric VTEC dynamics at these stations, not an artefact of the deterministic trend. The multifractal parameters obtained from the three GNSS stations point to a few consistent patterns. Across all stations, the singularity strength α_0 was small (Table 2), indicating that daily VTEC fluctuations are inher-

https://doi.org/10.5194/egusphere-2026-5194
Preprint. Discussion started: 4 September 2026

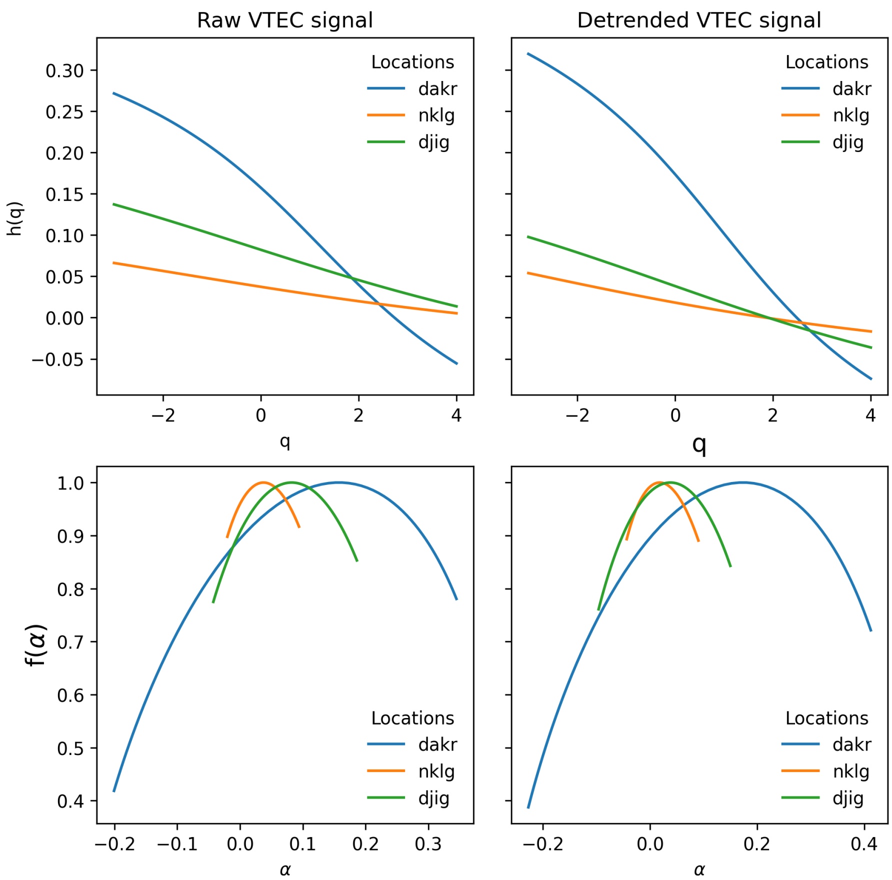

Figure 7. Multifractal scaling characteristics of daily minimum vTEC derived from MFDFA at the three GNSS stations. Upper panels: generalised Hurst exponent $h(q)$ as a function of moment order $q \in [-3, 4]$ for the raw (left) and STL-detrended (right) series. Lower panels: corresponding multifractal singularity spectra $f(\alpha)$ versus Hölder exponent α for the raw (left) and detrended (right) series.

ently rough and noise-like rather than smooth, and this became even more pronounced once the deterministic trend (diurnal, seasonal, and solar-cycle components) was removed. Specifically, at NKLG, and DJIG, the values of α_0 dropped close to zero after detrending, showing that most of their apparent structure came from the trend itself. DAKR behaved differently, keeping a comparatively high α_0 and, unusually, an even wider multifractal spectrum ($\Delta\alpha$) after detrending, suggesting that its complexity was not inherited from the seasonal cycle but reflects true intrinsic ionospheric variability, plausibly linked to its strategic position within the equatorial ionization anomaly region. The other two stations showed the opposite tendency, with maximum and minimum vTEC series converging toward similar $\Delta\alpha$ values once the trend was removed, implying that quiet and active periods share a comparable degree of underlying complexity when the predictable component is stripped away. The statistical significance parameter S confirms that the observed multifractality is robust at all stations in both series. For the maximum series, S ranges from 3.25 to 3.61 (raw) and 2.98 to 3.40 (detrended), while for the minimum series S ranges from 2.85 to

https://doi.org/10.5194/egusphere-2026-5194
Preprint. Discussion started: 4 September 2026

3.56, ruling out artefacts of sample size or finite-window effects. The singularity spectra for the minimum series are consistently narrower than their maximum counterparts. A notable asymmetry is observed at NKLG in the minimum series, where $r = 0.95$, indicating a near-symmetric spectrum with a slightly stronger contribution from large fluctuations to the multifractal structure than small fluctuations (Shimizu et al., 2002), whereas DAKR ($r = 0.80$) and DJIG ($r = 0.80$) remain left-skewed in both series. Following STL detrending, the $h(q)$ curves for NKLG, and DJIG become nearly flat in both the maximum and minimum series, and their singularity spectra narrow substantially, with all $\Delta\alpha < 0.20$ and $h(q = 2) \approx 0$. This confirms that most of the multifractal complexity in those series originates from the seasonal trend rather than from intrinsic ionospheric dynamics. DAKR stands apart in both series. Notwithstanding their closeness to the magnetic equator, the ionosphere over DAKR (at 2.35 magnetic latitude in West Africa) and DJIG (at 3.33 magnetic latitude in East Africa) exhibit marked differences in their multifractal scaling characteristics, a disparity we attribute to the significant longitudinal differences in the thermospheric neutral (zonal and meridional) wind observed at the west and east African equatorial sectors, which have been reported to be responsible for the longitudinal differences in equatorial electric fields between the west and east Africa stations (Rabiu et al., 2011, 2017, 2021; Jones et al., 2013; Maute et al., 2015; Okoh et al., 2022; Yizengaw et al., 2014). These results reveal a clear daytime-nighttime asymmetry in ionospheric scaling dynamics. The daytime ionosphere supports richer multifractal structure, stronger memory, and wider singularity spectra, while the nighttime ionosphere exhibits narrower and weaker multifractality consistent with a less dynamically active plasma in the absence of photo-ionisation. DAKR is the sole exception, sustaining nonlinear variability throughout the diurnal cycle owing to recurrent plasma depletions that persist independently of the seasonal trend at the EIA crest.

4 Conclusions

This study examined the multifractal scaling of daily maximum and minimum vTEC at three African GNSS stations spanning the equatorial ionisation anomaly (EIA) crest and its flanks over 2017–2019, using MFDFA on both raw and STL-detrended series to separate seasonal trend from intrinsic ionospheric dynamics. The raw maximum vTEC series showed genuine multifractality at all three stations, with $h(2)$ ranging from 0.104 to 0.193 and statistically significant spectral widths, along with a scale-dependent crossover near $n \approx 150$ days indicating stronger sub-annual persistence, particularly at DAKR and DJIG. The raw minimum series were also multifractal but consistently narrower and weaker in scaling, reflecting the reduced dynamical activity of the nighttime ionosphere relative to the solar-driven daytime regime. After STL detrending, multifractal complexity collapsed at NKLG, and DJIG in both series ($\Delta\alpha < 0.20$), showing that their scaling structure is largely seasonal rather than intrinsic. DAKR was the exception, retaining robust multifractality after detrending in both the maximum ($\Delta\alpha = 0.65$) and minimum ($\Delta\alpha = 0.64$) series, with extreme nighttime depletion events in 2017–2018 consistent with recurrent equatorial plasma bubbles characteristic of the West African sector. These results highlight the importance of detrending in ionospheric scaling analyses, identify the EIA crest as a physically distinct region where non-seasonal irregularities leave a measurable imprint on vTEC scaling, with implications for GNSS positioning error modelling and scintillation forecasting.

https://doi.org/10.5194/egusphere-2026-5194
Preprint. Discussion started: 4 September 2026

Acknowledgements. Conversion of geographical Coordinates to geomagnetic coordinates was done using the webpage of UK Solar System Data Centre (https://www.ukssdc.ac.uk/). BR would like to acknowledge support from the ICTP through the Associates Programme (2023–2028).

We express our gratitude to the International GNSS Service (IGS) for providing access to open-source GNSS data and orbit products. We also thank NASA's Crustal Dynamics Data Information System (CDDIS) for hosting the data archives, as well as the national agencies and station operators whose continuous monitoring infrastructure makes this research possible.

Code availability. Not applicable

Data availability. The GNSS observational data and satellite orbit products used in this study were provided by the International GNSS Service (IGS) and are publicly available through its Crustal Dynamics Data Information System (CDDIS) repository at https://cddis.nasa.gov/archive/gnss/data/ (or via the IGS Data Center network).

Author contributions. A.B.R. conceptualised the study and provided scientific supervision throughout. S.T.O. designed the methodology, developed and executed the computational analysis, and led the writing of the original draft. A.O. contributed to data curation, validation of results, and preparation of figures. All authors contributed to the interpretation of results, reviewed and edited the manuscript, and approved the final version for submission.

Competing interests. The authors declare that they have no conflict of interest.

References

Abdu, M.: Equatorial spread F/plasma bubble irregularities under storm time disturbance electric fields, Journal of atmospheric and solar-terrestrial physics, 75, 44–56, 2012.

Adebayo, O. M., Kherani, E. A., Pimenta, A. A., and Rabiu, B.: Pre-seismic ionospheric disturbances (PIDs) associated With 2021 Mw 7.5 Northern Peru earthquake: GNSS and ground uplift observations, Journal of Atmospheric and Solar-Terrestrial Physics, 277, 106 644, https://doi.org/https://doi.org/10.1016/j.jastp.2025.106644, 2025.

Adebesin, B., Rabiu, A., Adeniyi, J., and Amory-Mazaudier, C.: Nighttime morphology of vertical plasma drifts at Ouagadougou during different seasons and phases of sunspot cycles 20–22, Journal of Geophysical Research: Space Physics, 120, 10 020–10 038, 2015.

Akala, A. O., Rabiu, A. B., Somoye, E. O., Oyeyemi, E. O., and Adeloye, A. B.: The response of African equatorial GPS-TEC to intense geomagnetic storms during the ascending phase of solar cycle 24, Journal of Atmospheric and Solar-Terrestrial Physics, 98, 50–62, https://doi.org/10.1016/j.jastp.2013.02.006, 2013.

Anderson, D. N.: A theoretical study of the ionospheric F region equatorial anomaly, Journal of Geophysical Research, 78, 792–803, https://doi.org/10.1029/JA078i004p00792, 1973.

Andima, G., Amabayo, E. B., Jurua, E., and Cilliers, P. J.: Modeling of GPS total electron content over the African low-latitude region, Annales Geophysicae, 37, 65–76, https://doi.org/10.5194/angeo-37-65-2019, 2019.

Appleton, E. V.: Two anomalies in the ionosphere, Nature, 157, 691, https://doi.org/10.1038/157691a0, 1946.

Balan, N., Liu, L., and Le, H.: A brief review of equatorial ionization anomaly and ionospheric irregularities, Earth and Planetary Physics, 2, 257–275, https://doi.org/10.26464/epp2018025, 2018.

Bhardwaj, S., Chandrasekhar, E., and Gadre, V. M.: Characterization of ionospheric total electron content using wavelet-based multifractal formalism, Chaos, Solitons & Fractals, 134, 109 721, https://doi.org/10.1016/j.chaos.2020.109721, 2020.

Bianchi, S.: `fathon`: A Python package for a fast computation of detrendend fluctuation analysis and related algorithms, Journal of Open Source Software, 5, 1828, https://doi.org/10.21105/joss.01828, 2020.

Bolzan, M. J. A., Tardelli, A., Pillat, V. G., Fagundes, P. R., and Rosa, R. R.: Multifractal analysis of vertical total electron content (VTEC) at equatorial region and low latitude, during low solar activity, Annales Geophysicae, 31, 127–133, https://doi.org/10.5194/angeo-31-127-2013, 2013.

Chandrasekhar, E., Subhakar, D., Das, S. K., and Sharma, S.: Multifractal detrended fluctuation analysis of ionospheric total electron content data during solar minimum and maximum, Journal of Atmospheric and Solar-Terrestrial Physics, 149, 31–39, https://doi.org/10.1016/j.jastp.2016.09.007, 2016.

Cleveland, R. B., Cleveland, W. S., McRae, J. E., and Terpenning, I.: STL: A seasonal-trend decomposition procedure based on Loess, Journal of Official Statistics, 6, 3–73, 1990.

Feder, J.: Fractals, Springer Science & Business Media, New York, 2013.

Halsey, T. C., Jensen, M. H., Kadanoff, L. P., Procaccia, I., and Shraiman, B. I.: Fractal measures and their singularities: The characterization of strange sets, Physical Review A, 33, 1141–1151, https://doi.org/10.1103/PhysRevA.33.1141, 1986.

Hanson, W. B. and Moffett, R. J.: Ionization transport effects in the equatorial F region, Journal of Geophysical Research, 71, 5559–5572, https://doi.org/10.1029/JZ071i023p05559, 1966.

Hargreaves, J. K.: The Solar-Terrestrial Environment: An Introduction to Geospace – the Science of the Terrestrial Upper Atmosphere, Ionosphere, and Magnetosphere, Cambridge University Press, Cambridge, 1992.

Hernández-Pajares, M., Juan, J. M., Sanz, J., Orus, R., Garcia-Rigo, A., Feltens, J., Komjathy, A., Schaer, S. C., and Krankowski, A.: The IGS VTEC maps: a reliable source of ionospheric information since 1998, Journal of Geodesy, 83, 263–275, https://doi.org/10.1007/s00190-008-0266-1, 2009.

Jakowski, N., Mayer, C., Hoque, M. M., and Wilken, V.: Total electron content models and their use in ionosphere monitoring, Radio Science, 46, RS0D18, https://doi.org/10.1029/2010RS004620, 2011.

Jones, Jr., M., Forbes, J. M., Hagan, M. E., and Maute, A.: Non-migrating tides in the ionosphere-thermosphere: In situ versus tropospheric sources, Journal of Geophysical Research, 118, 2438–2451, https://doi.org/10.1002/jgra.50257, 2013.

Kantelhardt, J. W.: Fractal and Multifractal Time Series, in: Encyclopedia of Complexity and Systems Science, edited by Meyers, R. A., pp. 3754–3779, Springer, New York, https://doi.org/10.1007/978-0-387-30440-3_221, 2009.

Kantelhardt, J. W., Zschiegner, S. A., Koscielny-Bunde, E., Havlin, S., Bunde, A., and Stanley, H. E.: Multifractal detrended fluctuation analysis of nonstationary time series, Physica A: Statistical Mechanics and its Applications, 316, 87–114, https://doi.org/10.1016/S0378-4371(02)01383-3, 2002.

Kelley, M. C.: The Earth's ionosphere: Plasma physics and electrodynamics, vol. 96, Academic press, 2nd edn., 2009.

Kuo, C. L., Lee, L. C., and Huba, J. D.: An improved coupling model for the lithosphere-atmosphere-ionosphere system, Journal of Geophysical Research: Space Physics, 119, 3189–3205, https://doi.org/https://doi.org/10.1002/2013JA019392, 2014.

Lieberman, R., Oberheide, J., Jones Jr, M., Siddiqui, T., Maute, A., Pedatella, N., Liu, A., and Klenzing's, J.: The influence of atmospheric tides on the variability of the mesosphere–thermosphere-ionosphere, Surveys in Geophysics, pp. 1–47, 2026.

Liu, L., Wan, W., Ning, B., Pirog, O., and Kurkin, V.: Solar activity variations of the ionospheric peak electron density, Journal of Geophysical Research: Space Physics, 111, 304, 2006.

Mannucci, A. J., Wilson, B. D., Yuan, D.-N., Ho, C. H., Lindqwister, U. J., and Runge, T. F.: A global mapping technique for GPS-derived ionospheric total electron content measurements, Radio Science, 33, 565–582, https://doi.org/10.1029/97RS02707, 1998.

Maute, A., Hagan, M. E., Yudin, V., Liu, H.-L., and Yizengaw, E.: Causes of the longitudinal differences in the equatorial vertical E×B drift during the 2013 SSW period as simulated by the TIME-GCM, Journal of Geophysical Research: Space Physics, 120, 5117–5136, https://doi.org/10.1002/2015JA021126, 2015.

Mendillo, M.: Storms in the ionosphere: Patterns and processes for total electron content, Reviews of Geophysics, 44, 2006.

Moffett, R. J. and Hanson, W. B.: Effect of ionization transport on the equatorial F region, Nature, 206, 705–706, https://doi.org/10.1038/206705a0, 1965.

Momeni, M. and Migoya-Orué, Y.: Multifractal insights into mid-latitude atmospheric and solar dynamics across different solar cycle phases, Advances in Space Research, 77, 2614–2636, https://doi.org/10.1016/j.asr.2025.10.108, 2026.

Muniafu, W., Uluma, E., and Lomotey, S. O.: Storm-time variability of GNSS-derived ionospheric VTEC over East Africa during four major geomagnetic storms of solar cycle 24, Earth and Planetary Science, 5, 3205, https://doi.org/10.36956/eps.v5i1.3205, 2026.

Nanda, K., Mondal, D., Sasmal, S., Hobara, Y., Maurya, A. K., Hayakawa, M., Potirakis, S. M., and Datta, A.: Atmospheric Impact of Typhoon Hagibis: A Multi-Layer Investigation of Stratospheric and Ionospheric Responses, Atmosphere, 17, https://doi.org/10.3390/atmos17020167, 2026.

Obasanjo, P., Okoh, D., Awuor, A., Baki, P., and Ochieng, G.: Multi-scale GNSS-TEC and GIM investigation of ionospheric perturbations triggered by the 28 March 2025 Myanmar earthquake preceded by geomagnetic storm, Frontiers in Astronomy and Space Sciences, 13, 1791 135, 2026.

Ogunjo, S.: Effect of data transformation on long term memory of chaotic time series, The African Review of Physics, 10, 2015.

Ogunjo, S., Rabiu, A., Fuwape, I., and Obafaye, A.: Evolution of Dynamical Complexities in Geospace as Captured by Dst Over Four Solar Cycles 1964–2008., Journal of Geophysical Research: Space Physics, 126, e2020JA027 873, 2021.

Ogunjo, S., Akinsusi, J., Rabiu, B., and Fuwape, I.: Dynamical complexity and multifractal analysis of geomagnetic activities at high temporal scales over three solar cycles, Journal of Atmospheric and Solar-Terrestrial Physics, 265, 106 380, https://doi.org/10.1016/j.jastp.2024.106380, 2024a.

Ogunjo, S., Rabiu, B., Fuwape, I., and Atikekeresola, O.: Multifractal and chaotic characteristics of geomagnetic inter-storm interval over eight solar cycles, Advances in Space Research, 73, 5406–5413, https://doi.org/10.1016/j.asr.2024.02.050, 2024b.

Ogwala, A., Habarulema, J. B., and Seemala, G. K.: Longitudinal variations in equatorial ionospheric TEC from GPS, global ionosphere map and International Reference Ionosphere-2016 during the descending and minimum phases of solar cycle 24, Universe, 8, 575, https://doi.org/10.3390/universe8110575, 2022.

Okoh, D., Seemala, G., Rabiu, B., Habarulema, J. B., Jin, S., Shiokawa, K., Otsuka, Y., Aggarwal, M., Uwamahoro, J., and Migoya-Orué, Y.: A neural network-based ionospheric model over Africa from Constellation Observing System for Meteorology, Ionosphere, and Climate and ground Global Navigation Satellite System observations, Journal of Geophysical Research: Space Physics, 124, 10 512–10 532, https://doi.org/10.1029/2019JA027065, 2019.

Okoh, D., Habarulema, J. B., Rabiu, B., Seemala, G., Nava, B., Cesaroni, C., Baki, P., and Migoya-Orué, Y.: Storm-time modeling of the African regional ionospheric total electron content using artificial neural networks, Space Weather, 18, e2020SW002 525, https://doi.org/10.1029/2020SW002525, 2020.

Okoh, D. I., Bounhir, A., Habarulema, J. B., Rabiu, B., Katamzi-Joseph, Z., Ojo, T., Wu, Q., and Makela, J. J.: Thermospheric Neutral Wind Measurements and Investigations across the African Region – A Review, Atmosphere, 13, 863, https://doi.org/10.3390/atmos13060863, 2022.

Olabode, A. O. and Ariyibi, E. A.: Geomagnetic storm main phase effect on the equatorial ionosphere over Ile–Ife as measured from GPS observations, Scientific African, 9, e00 472, https://doi.org/10.1016/j.sciaf.2020.e00472, 2020.

Olwendo, J. O., Cilliers, P. J., Baki, P., and Mito, C.: A study on the variability of ionospheric total electron content over the East African low-latitude region and storm time ionospheric variations, Radio Science, 51, 1503–1517, https://doi.org/10.1002/2015RS005785, 2016.

Opio, P., Habarulema, J. B., and Jurua, E.: Latitudinal variation of the ionosphere in the African sector using GPS TEC data, Advances in Space Research, 55, 1640–1650, https://doi.org/10.1016/j.asr.2014.12.036, 2015.

Peng, C.-K., Buldyrev, S. V., Havlin, S., Simons, M., Stanley, H. E., and Goldberger, A. L.: Mosaic organization of DNA nucleotides, Physical Review E, 49, 1685–1689, https://doi.org/10.1103/PhysRevE.49.1685, 1994.

Pulinets, S. and Dimitar, O.: Lithosphere–Atmosphere–Ionosphere Coupling (LAIC) model – An unified concept for earthquake precursors validation, Journal of Asian Earth Sciences, 41, 371–382, https://doi.org/https://doi.org/10.1016/j.jseaes.2010.03.005, validation of Earthquake Precursors-VESTO, 2011.

Rabiu, A., Yumoto, K., Falayi, E., Bello, O., and Group, C.: Ionosphere over Africa: Results from geomagnetic field measurements during International Heliophysical Year IHY, Journal of Sun and Geosphere, 6, 61–64, 2011.

Rabiu, A., Okoh, D., Wu, Q., Bolaji, O., Abdulrahim, R., Dare-Idowu, O., and Obafaye, A.: Investigation of the variability of night-time equatorial thermospheric winds over Nigeria, West Africa, Journal of Geophysical Research: Space Physics, 126, e2020JA028 528, 2021.

Rabiu, A. B., Folarin, O. O., Uozumi, T., Abdul Hamid, N. S., and Yoshikawa, A.: Longitudinal variation of equatorial electrojet and the occurrence of its counter electrojet, in: Annales Geophysicae, vol. 35, pp. 535–545, Copernicus Publications Göttingen, Germany, 2017.

Rishbeth, H.: How the thermospheric circulation affects the ionospheric F2-layer, Journal of Atmospheric and Solar-Terrestrial Physics, 60, 1385–1402, 1998.

Schaer, S.: Mapping and Predicting the Earth's Ionosphere Using the Global Positioning System, Ph.D. thesis, University of Bern, Bern, Switzerland, 1999.

Schreiber, T. and Schmitz, A.: Improved surrogate data for nonlinearity tests, Physical Review Letters, 77, 635–638, https://doi.org/10.1103/PhysRevLett.77.635, 1996.

Schunk, R. W. and Nagy, A. F.: Ionospheres: Physics, plasma physics, and chemistry, Cambridge University Press, 2009.

Shimizu, Y., Thurner, S., and Ehrenberger, K.: Multifractal spectra as a measure of complexity in human posture, Fractals, 10, 103–116, 2002.

Sivavaraprasad, G., Otsuka, Y., Tripathi, N. K., Chowdhary, V. R., Ratnam, D. V., and Khan, M. A.: Spatial and temporal characteristics of ionospheric total electron content over Indian equatorial and low-latitude GNSS stations, in: 2018 Conference on Signal Processing And Communication Engineering Systems (SPACES), pp. 105–108, IEEE, 2018.

Tanna, H. and Pathak, K.: Multifractality due to long-range correlation in the L-band ionospheric scintillation S 4 index time series, Astrophysics and Space Science, 350, 47–56, 2014a.

Tanna, H. and Pathak, K.: Multifractal behaviour of the ionospheric scintillation index time series over an Indian low latitude station Surat, Journal of Atmospheric and Solar-Terrestrial Physics, 109, 66–74, https://doi.org/https://doi.org/10.1016/j.jastp.2014.01.009, 2014b.

Theiler, J., Eubank, S., Longtin, A., Galdrikian, B., and Farmer, J. D.: Testing for nonlinearity in time series: The method of surrogate data, Physica D: Nonlinear Phenomena, 58, 77–94, https://doi.org/10.1016/0167-2789(92)90102-S, 1992.

Uga, C. I., Uluma, E., Adhikari, B., Giri, A., and Belay, N.: Impact of the October 28, 2021 Solar Flare and the November 4, 2021 Geomagnetic Storm on the Low, Middle, and High-Latitude Ionosphere, Discover Space, 128, 4, https://doi.org/10.1007/s11038-024-09556-6, 2024.

Yizengaw, E., Moldwin, M., Zesta, E., Biouele, C., Damtie, B., Mebrahtu, A., Rabiu, B., Valladares, C., and Stoneback, R.: The longitudinal variability of equatorial electrojet and vertical drift velocity in the African and American sectors, in: Annales Geophysicae, vol. 32, pp. 231–238, Copernicus Publications Göttingen, Germany, 2014.

https://doi.org/10.5194/egusphere-2026-5194
Preprint. Discussion started: 4 September 2026

Table 2. Generalized Hurst exponent (h), linear-fit parameters (a_0, a, r), and scaling-range width (S) obtained from MFDFA of the raw and detrended daily maximum and minimum VTEC series at $q = 2$, for the full series and its first and second halves, at the three GNSS stations.

			Generalized Hurst exponent, h						Multifractal statistics						S	
			Raw			Detrended			Raw			Detrended				
	Station	q	h_{full}	$h_{\text{1st half}}$	$h_{\text{2nd half}}$	h_{full}	$h_{\text{1st half}}$	$h_{\text{2nd half}}$	α_0	$\Delta\alpha$	r	α_0	$\Delta\alpha$	r	Raw	Det.
VTEC max	DAKR	2	0.127	0.306	0.044	0.041	0.111	0.024	0.22	0.46	0.49	0.20	0.65	0.60	3.25	3.23
	NKLG	2	0.182	0.315	0.089	-0.001	0.027	-0.006	0.20	0.11	0.58	0.02	0.11	0.80	3.38	3.02
	DJIG	2	0.193	0.398	0.074	0.003	0.017	-0.001	0.23	0.19	0.59	0.03	0.17	0.77	3.43	3.40
VTEC min	DAKR	2	0.040	0.047	0.033	0.031	0.038	0.028	0.16	0.55	0.50	0.18	0.64	0.57	3.10	3.16
	NKLG	2	0.020	0.076	0.005	-0.001	0.030	-0.007	0.04	0.11	0.95	0.02	0.13	1.13	3.47	3.46
	DJIG	2	0.046	0.109	0.025	-0.002	0.050	-0.009	0.08	0.23	0.80	0.04	0.25	0.81	2.98	2.94

S represents the statistical significance of α ($\alpha > 2$, is statistically significant)